euronoise 2021
25th to 27th of October
Madeira, Portugal - online

Spiraling waves and detection of phase singularities in objects immersed in inhomogeneous acoustic fields

Ludovic Alhaïtz*, Diego Baresch, Thomas Brunet, Christophe Aristégui, Olivier Poncelet

Univ. Bordeaux, CNRS, Bordeaux INP, UMR 5295 I2M, Talence, France.

*{ludovic.alhaitz@u-bordeaux.fr}

Abstract

We report experimental developments on the scattering of acoustic evanescent waves by an isolated particle. Compared to the scattering of homogeneous plane waves, additional oscillation modes are excited and particularly lead to the generation of spiraling scattered waves propagating angularly in the far field. Interestingly, phase singularities may appear inside the scattering particle as a consequence of interfering circumferential waves. The topological charge of these singular waves depends on the targeted scattered mode, excited by adjusting the driving frequency for a fixed particle size. We conducted experiments at ultrasonic frequencies on a resonant droplet immersed in a non-miscible host fluid to evidence these topological singularities. Evanescent waves were generated by total reflection at a two fluid interface at which the droplet was closely deposited. The field resulting from the scattering is shown to carry a transverse angular momentum of orbital nature which could bring an additionnal degree of freedom than classical vortex beams. Furthermore, the emergence of topological singularities in the field could be also linked to an acoustic spin density, important for applications involving radiation force and torque.

Keywords: evanescent waves, scattering, spiraling waves, phase singularities.

1 Introduction

Evanescent waves are inhomogeneous waves naturally occuring in wave fields and are known to possess peculiar properties [1]. They could be exploited for applications in optics or acoustics such as particle manipulation [2, 3] or imaging [4, 5]. For several decades, the angular momentum carried by acoustic fields has been the subject of many studies for its importance in many practical applications [6, 7, 8, 9]. Importantly, it has been demonstrated that the transfert of orbital angular momentum to an absorbing particle leads to the application of a radiation torque on this particle [10, 11, 12, 13]. Recent studies also examined theoretically the radiation force and torque induced by the scattering of evanescent waves in acoustics [14].

In this experimental work, we focus on the scattering of ultrasonic evanescent waves by resonant droplets and analyse the structure of the resulting field. It has been noticed that the asymmetry of the incident wave alters considerably the field structure compared to an homogenous wave [15]. More precisely, due to the amplitude gradient in the evanescent pressure field, the scattering particle is free to vibrate both in the propagation direction and in the transversal direction, the latter being amplified when the evanescence of the incident wave increases. It will be shown that the resulting scattered and internal fields carry an orbital angular momentum linked to the apperaence of phase singularities inside the particle.

Firstly, the experimental set-up for the generation of evanescent waves and acoustic measurements is presented. Then, several measurements of the field outside and inside a resonant droplet are analysed with particular emphasis on the angular momentum arising in such a field.

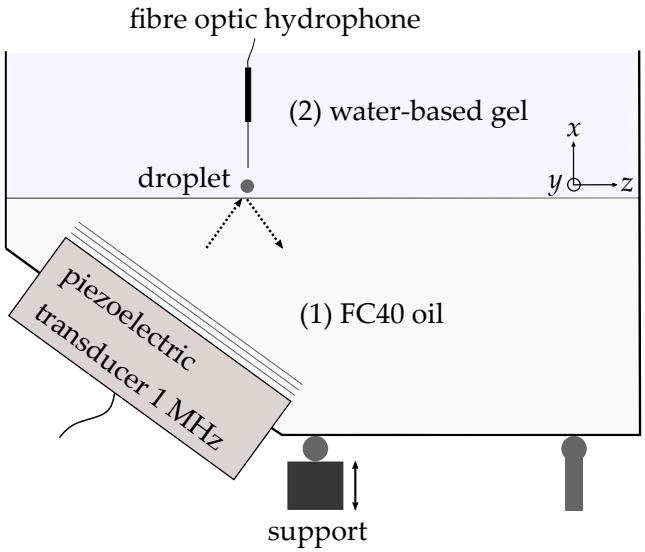

Figure 1: (a) Experimental set-up for the generation of evanescent waves and scattering measurements.

2 Generation of evanescent waves and scattering measurements

Ultrasonic waves were generated by a broadband longitudinal wave transducer, having a central frequency of 1 MHz, immersed in a tank. The apparatus is shown in Fig. 1 and is similar to [16]. Evanescent waves were generated by total internal reflection at a two-fluid interface. To adjust the angle of incidence, the water tank can be tilted using a vertical translation stage combined with a pivot linkage. To stabilize a particle in a fixed position near the interface, we used carbopol as a suspending fluid [17, 18]. It is a water-based gel advantageously combining acoustic properties very similar to water with a yield stress sufficient to avoid droplet sedimentation. The transducer is placed in a F40 oil medium (1) which is denser and has a lower sound speed than carbopol (2), necessary to achieve reflection beyond a critical angle and generate an evanescent wave in the water phase. These two fluid are immiscible and their properties are summarised in the table 1. The critical angle of transmission for this configuration is equal to 25.3°. Acoustic field measurements were performed

	mass density (kg/m^3)	longitudinal celerity (m/s)
carbopol	1050	1500
FC40 oil	1850	640

Table 1: Acoustic properties of the fluids used in the experiments.

by using a fibre optic hydrophone (10 micron sensitive area). The experimental set-up is presented in Fig. 1 and the frequency range [0.5 − 1.5] Mhz set by the bandwidth was explored. Fig. 2 (a) shows an example of evanescent field that has been measured in medium (1), and obtained from the reflexion of a 1 MHz pulse. It propagates along the direction of the interface, z, and decays in amplitude in the orthogonal direction, x. It can be described by a complex-valued wave vector $\mathbf{k}_{\text{inc}} = k_z\mathbf{z} + \mathrm{i}\kappa\mathbf{x}$, where k_z is the propagation wave number and κ is the decay rate in amplitude in the orthogonal direction. The spatial part of the pressure field can be expressed as follows:

$$p = p_0\, \mathrm{e}^{\mathrm{i}k_z z - \kappa x}, \tag{1}$$

where p_0 is a constant amplitude. The amplitude of the field along the vertical direction indicated by the dotted line in Fig. 2 (a) is plotted in Fig. 2 (b). The amplitude decay can be fitted by an exponential function and the ratio between the imaginary part and the real part of the wave vector $\mathbf{k}_{\text{inc}}$ is here equal to 0.45.

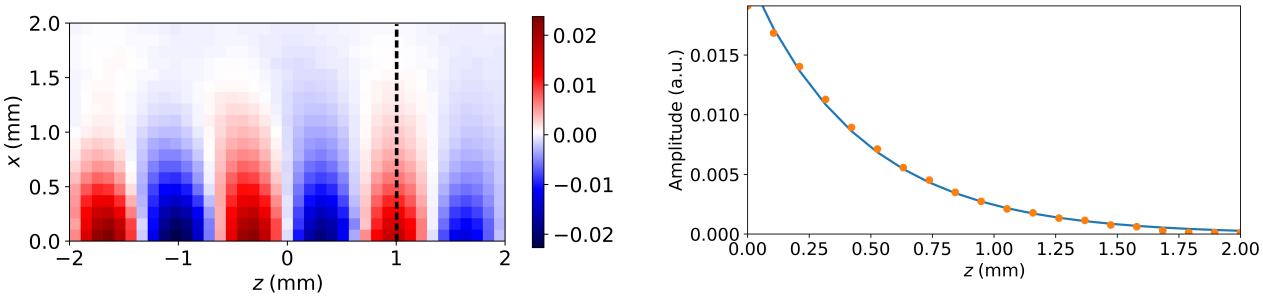

(a) (b)

Figure 2: (a) Spatial map of the pressure field measured from a 1 MHz signal. (b) Evolution of the amplitude of the field along the black dotted line in (a). The measurement points in orange can be fitted by an exponential decay in the vertical direction.

3 Spiraling scattered waves and detection of phase singularities inside a droplet

Next, the evanescent waves were made to interact with FC 40 droplets suspended in fluid (2). These droplets exhibit strong Mie resonances because of a high acoustic contrast with water or carbopol [17, 18]. Single droplets were positioned close to the interface using a syringe. Fig. 3 shows a spatial map of the pressure field outside a droplet of diameter $d = 0.88$ mm in the (xz)-plane centered on the droplet. The central frequency of the incident signal $f_0 = 0.81$ MHz corresponds to the dipolar resonance frequency of the droplet. Note that it is sub-wavelength in size compared to waves propagating in the carbopol $d < \lambda = 1.85$ mm. The incident evanescent wave propagates from the left to the right and we clearly see the scattered field above the droplet where the incident wave fades away. Due to symmetry breaking effects occuring in the scattering of an evanescent wave, waves propagating angularly along the particle circonference are selected by increasing the evanescence. As a result, these waves radiate outwards with a spiral-shaped wavefront as reported in a previous analytical study [15]. In addition, as the field is circular, its directivity above the droplet is almost isotropic, which could be interesting in imaging applications [19]. As the phase of the scattered field varies angularly, it carries an orbital angular momentum density in the transversal direction, y. Importantly, this differs from the case of acoustic vortex beams, where the wavefront spirals around the propagation direction with which the angular momentum density is aligned [6].

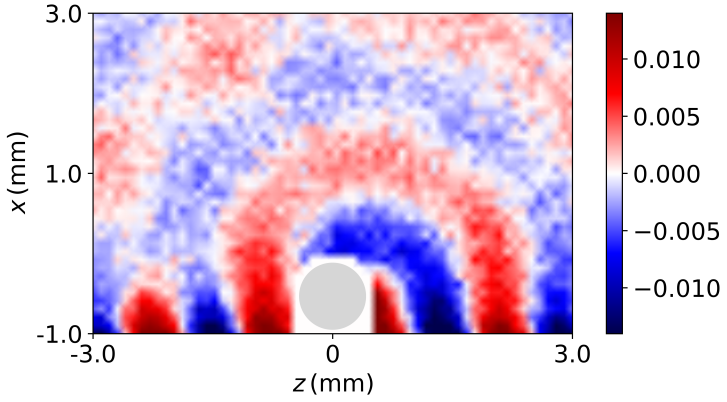

Figure 3: (a) Pressure field in the (xz)-plane outside a FC40 oil droplet of 0.88 mm diameter. The central pulse frequency, $f = 0.81$ MHz, excites the dipolar resonance of the droplet.

Based on observations of the field in the exterior medium, we investigated the structure of the field inside

the particle. The droplet was positioned near the interface first and the hydrophone was inserted vertically in the droplet in a second step. A map of the internal field was obtained by gently displacing the hydrophone within the droplet (Fig. 4 (a)). In order to restrain its displacement when the optical fibre is translated through it, a bigger droplet of diamater $d = 2.23$ mm was injected. As wee can see on the photo, the droplet slightly loses its sphericity because of the contact with the fibre, but without inducing any measurable effect on the field properties. Fig. 4 (b) shows the phase of the internal pressure field in the (xz)-plane at a frequency $f = 0.535$ MHz corresponding to the hexapolar resonance of the particle. On the left, the field has been computed from the Mie scattering theory of evanescent waves by spherical objects introduced in [15]. The insets on the right show the phase and modulus of the field measured at the same frequency. Interestingly, phase singularities may appear inside the particle as a consequence of destructive interferences between cicumferential waves confined at the droplet surface and radiating spiraling waves outwards. The position of each singularity matches well with the model. One can notice that the topological charge of the field, which corresponds to the number of 2π phase jumps following a circular path around the droplets centre, depends on the targeted scattered mode (hexapolar), fixed by the particle size and driving frequency.

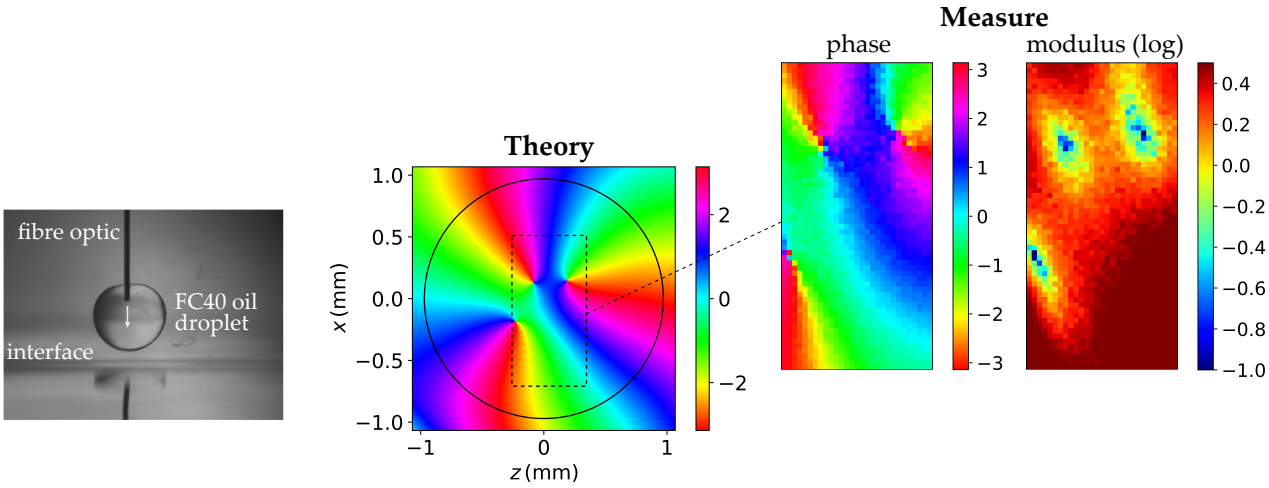

(a) (b)

Figure 4: (a) Photograph of a FC40 oil droplet placed near the interface between carbopol and FC40 oil. (b) Pressure field in the (xz)-plane inside a droplet of 2.23 mm diameter: phase of the predicted field (left) / phase and modulus (log scale) of the measured field (right). The central pulse frequency, $f = 0.535$ MHz, excites the hexapolar resonance of the droplet.

4 Conclusions

A spiral scattering regime resulting from the interation between an acoustic evanescent wave and a spherical object has been observed experimentally. It has been shown that phase singularities may appear inside a resonant droplet and the number of singular points corresponds to the order of the preferentially excited scattering mode. These two features are linked to a transverse orbital angular momentum carried by the field, which offers an additional degree of freedom for the control of wave propagation from that of usual vortex beams and could result useful for further applications. Importantly, the existence of a spin density in inhomogeneous acoustic fields has been recently introduced and quantify the local rotation of the particle velocity vector field [9, 20, 21, 22]. It will be considered in future studies and could have important implications for the control of particle rotation.

References

[1] Konstantin Y Bliokh, Aleksandr Y Bekshaev, and Franco Nori. Extraordinary momentum and spin in evanescent waves. *Nature communications*, 5(1):1–8, 2014.

[2] Antoine Canaguier-Durand and Cyriaque Genet. Transverse spinning of a sphere in a plasmonic field. *Physical Review A*, 89(3):033841, 2014.

[3] Vivian Aubert, Régis Wunenburger, Tony Valier-Brasier, David Rabaud, Jean-Philippe Kleman, and Cédric Poulain. A simple acoustofluidic chip for microscale manipulation using evanescent scholte waves. *Lab on a Chip*, 16(13):2532–2539, 2016.

[4] Paul Bazylewski, Sabastine Ezugwu, and Giovanni Fanchini. A review of three-dimensional scanning near-field optical microscopy (3d-snom) and its applications in nanoscale light management. *Applied Sciences*, 7(10):973, 2017.

[5] Chu Ma, Seok Kim, and Nicholas X Fang. Far-field acoustic subwavelength imaging and edge detection based on spatial filtering and wave vector conversion. *Nature communications*, 10(1):1–10, 2019.

[6] Brian T Hefner and Philip L Marston. An acoustical helicoidal wave transducer with applications for the alignment of ultrasonic and underwater systems. *The Journal of the Acoustical Society of America*, 106(6):3313–3316, 1999.

[7] Jean-Louis Thomas and Régis Marchiano. Pseudo angular momentum and topological charge conservation for nonlinear acoustical vortices. *Physical review letters*, 91(24):244302, 2003.

[8] John Lekner. Acoustic beams with angular momentum. *The Journal of the Acoustical Society of America*, 120(6):3475–3478, 2006.

[9] Konstantin Y Bliokh and Franco Nori. Spin and orbital angular momenta of acoustic beams. *Physical Review B*, 99(17):174310, 2019.

[10] Likun Zhang and Philip L Marston. Angular momentum flux of nonparaxial acoustic vortex beams and torques on axisymmetric objects. *Physical Review E*, 84(6):065601, 2011.

[11] Glauber T Silva. Acoustic radiation force and torque on an absorbing compressible particle in an inviscid fluid. *The Journal of the Acoustical Society of America*, 136(5):2405–2413, 2014.

[12] Likun Zhang. Reversals of orbital angular momentum transfer and radiation torque. *Physical Review Applied*, 10(3):034039, 2018.

[13] Diego Baresch, Jean-Louis Thomas, and Régis Marchiano. Orbital angular momentum transfer to stably trapped elastic particles in acoustical vortex beams. *Physical review letters*, 121(7):074301, 2018.

[14] ID Toftul, KY Bliokh, Mihail I Petrov, and Franco Nori. Acoustic radiation force and torque on small particles as measures of the canonical momentum and spin densities. *Physical review letters*, 123(18):183901, 2019.

[15] Ludovic Alhaïtz, Diego Baresch, Thomas Brunet, Christophe Aristégui, and Olivier Poncelet. Spiral-shaped scattered field from incident evanescent acoustic waves on a mie particle. *Journal of Physics: Conference Series*, 1761(1):012003, 2021.

[16] Curtis F Osterhoudt, David B Thiessen, Scot F Morse, and Philip L Marston. Evanescent acoustic waves from subcritical beam illumination: Laboratory measurements near a liquid–liquid interface. *IEEE Journal of Oceanic Engineering*, 33(4):397–404, 2008.

[17] Benoit Mascaro, Thomas Brunet, Olivier Poncelet, Christophe Aristégui, Simon Raffy, Olivier Mondain-Monval, and Jacques Leng. Impact of polydispersity on multipolar resonant scattering in emulsions. *The Journal of the Acoustical Society of America*, 133(4):1996–2003, 2013.

[18] Benoit Tallon, Thomas Brunet, Jacques Leng, and John H Page. Energy velocity of multiply scattered waves in strongly scattering media. *Physical Review B*, 101(5):054202, 2020.

[19] Daniel S Plotnick, Timothy M Marston, and Philip L Marston. Circular synthetic aperture sonar imaging

of simple objects illuminated by an evanescent wavefield. *The Journal of the Acoustical Society of America*, 140(4):2839–2846, 2016.

[20] Chengzhi Shi, Rongkuo Zhao, Yang Long, Sui Yang, Yuan Wang, Hong Chen, Jie Ren, and Xiang Zhang. Observation of acoustic spin. *National Science Review*, 2019.

[21] Konstantin Y Bliokh and Franco Nori. Transverse spin and surface waves in acoustic metamaterials. *Physical Review B*, 99(2):020301, 2019.

[22] Yang Long, Danmei Zhang, Chenwen Yang, Jianmin Ge, Hong Chen, and Jie Ren. Realization of acoustic spin transport in metasurface waveguides. *Nature communications*, 11(1):1–7, 2020.